

MIT OpenCourseWare
<http://ocw.mit.edu>

5.80 Small-Molecule Spectroscopy and Dynamics
Fall 2008

For information about citing these materials or our Terms of Use, visit: <http://ocw.mit.edu/terms>.

Lecture # 8 Supplement

Contents

1.	Excerpts from The Spectra and Dynamics of Diatomic Molecules	1
2.	Electronic Configurations	2

1. Excerpts from The Spectra and Dynamics of Diatomic Molecules

**by Professor Robert W. Field
and Hélène Lefebvre-Brion**

Elsevier Academic Press

2004

Chapter 3

Terms Neglected in the Born-Oppenheimer Approximation

Contents

3.1	The Born-Oppenheimer Approximation	89
3.1.1	Potential Energy Curves	90
3.1.2	Terms Neglected in the Born-Oppenheimer Approximation	92
3.1.2.1	Electrostatic and Nonadiabatic Part of \mathbf{H}	92
3.1.2.1.1	Crossing or Diabatic Curves	93
3.1.2.1.2	Noncrossing or Adiabatic Curves	94
3.1.2.2	The Spin Part of \mathbf{H}	94
3.1.2.3	Rotational Part of \mathbf{H}	96
3.2	Basis Functions	99
3.2.1	Hund's Cases	101
3.2.1.1	Definition of Basis Sets	103
3.2.1.2	Quantum Numbers, Level Patterns, and the Effects of Terms Excluded from $\mathbf{H}^{(0)}$	113
3.2.1.3	Intermediate Case Situations	126
3.2.1.3.1	Introduction	126
3.2.1.3.2	Examples	127
3.2.1.4	Transformations Between Hund's Case Basis Sets	130
3.2.1.5	Spectroscopic vs. Dynamical Hund's Cases	136
3.2.1.6	Relationship between Noncommuting Terms in \mathbf{H} and the Most Appropriate Hund's Case	137
3.2.2	Symmetry Properties	138

3.2.2.1	Symmetry Properties of Hund's Case (a) Basis Functions	138
3.2.2.2	Symmetry Properties of non-Hund's Case (a) Basis Functions	146
3.2.3	Molecular Electronic Wavefunctions	148
3.2.4	Matrix Elements between Electronic Wavefunctions	156
3.3	Electrostatic Perturbations	161
3.3.1	Diabatic Curves	163
3.3.2	Approximate Representation of the Diabatic Elec- tronic Wavefunction	165
3.3.3	Adiabatic Curves	168
3.3.4	Choice between the Diabatic and Adiabatic Models .	172
3.3.5	Electromagnetic Field-Dressed Diabatic and Adia- batic Potential Energy Curves	177
3.4	Spin Part of the Hamiltonian	180
3.4.1	The Spin-Orbit Operator	181
3.4.2	Expression of Spin-Orbit Matrix Elements in Terms of One-Electron Molecular Spin-Orbit Parameters .	183
3.4.2.1	Matrix Elements of the $\mathbf{I}_{zi} \cdot \mathbf{s}_{zi}$ Term . . .	183
3.4.2.1.1	Diagonal Matrix Elements	183
3.4.2.1.2	Off-Diagonal Matrix Elements	187
3.4.2.2	Matrix Elements of the $(\mathbf{I}_i^+ \mathbf{s}_i^- + \mathbf{I}_i^- \mathbf{s}_i^+)$ Part of \mathbf{H}^{SO}	190
3.4.3	The Spin-Rotation Operator	191
3.4.4	The Spin-Spin Operator	196
3.4.4.1	Diagonal Matrix Elements of \mathbf{H}^{SS} ; Calcu- lation of the Direct Spin-Spin Parameter .	196
3.4.4.2	Calculation of Second-Order Spin-Orbit Ef- fects	198
3.4.4.2.1	π^2 Configuration	201
3.4.4.2.2	$\pi^3 \pi'$ (or $\pi^3 \pi'^3$ and $\pi \pi'$) Configu- rations	201
3.4.4.3	Off-Diagonal Matrix Elements	202
3.4.5	Tensorial Operators	203
3.5	Rotational Perturbations	210
3.5.1	Spin-Electronic Homogeneous Perturbations	210
3.5.2	The \mathbf{S} -Uncoupling Operator	212
3.5.3	The \mathbf{L} -Uncoupling Operator	213
3.5.4	${}^2\Pi \sim {}^2\Sigma^+$ Interaction	217
3.6	References	227

3.1 The Born-Oppenheimer Approximation

The exact Hamiltonian \mathbf{H} for a diatomic molecule, with the electronic coordinates expressed in the molecule-fixed axis system, is rather difficult to derive. Bunker (1968) provides a detailed derivation as well as a review of the coordinate conventions, implicit approximations, and errors in previous discussions of the exact diatomic molecule Hamiltonian.

Our goal is to find the exact solutions, ψ_i^T ($T = \text{Total}$), of the Schrödinger equation,

$$\mathbf{H}\psi_i^T = E_i^T \psi_i^T, \quad (3.1.1)$$

which correspond to the observed (exact) E_i^T energy levels. \mathbf{H} is the nonrelativistic Hamiltonian, which may be approximated by a sum of three operators,

$$\mathbf{H} = \mathbf{T}^N(R, \theta, \phi) + \mathbf{T}^e(r) + V(r, R), \quad (3.1.2)$$

where \mathbf{T}^N is the nuclear kinetic energy, \mathbf{T}^e is the electron kinetic energy, V is the electrostatic potential energy for the nuclei and electrons (including $e^- - e^-$, $e^- - N$ and $N - N$ interactions), R is the internuclear distance, θ and ϕ specify the orientation of the internuclear axis (molecule-fixed coordinate system) relative to the laboratory coordinate system (see Section 2.3.3 and Fig. 2.4), and r represents all electron coordinates in the molecule-fixed system.

The nuclear kinetic energy operator is given by

$$\mathbf{T}^N(R, \theta, \phi) = \frac{-\hbar^2}{2\mu R^2} \left[\frac{\partial}{\partial R} \left(R^2 \frac{\partial}{\partial R} \right) + \frac{1}{\sin \theta} \frac{\partial}{\partial \theta} \left(\sin \theta \frac{\partial}{\partial \theta} \right) + \frac{1}{\sin^2 \theta} \frac{\partial^2}{\partial \phi^2} \right], \quad (3.1.3a)$$

where

$$\mu = \frac{M_A M_B}{M_A + M_B}$$

is the nuclear reduced mass, with M_A and M_B the masses of atoms A and B. \mathbf{T}^N can be divided into vibrational and rotational terms,

$$\mathbf{T}^N(R, \theta, \phi) = \mathbf{T}^N(R) + \mathbf{H}^{ROT}(R, \theta, \phi). \quad (3.1.3b)$$

The electron kinetic energy operator is

$$\mathbf{T}^e(r) = \frac{-\hbar^2}{2m} \sum_i \nabla_i^2, \quad (3.1.3c)$$

where m is the electron mass and the summation is over all n electrons.[†]

[†]The part of \mathbf{T}^e ,

$$\frac{-\hbar^2}{2(M_A + M_B)} \sum_{i,j} \nabla_i \nabla_j,$$

the diagonal matrix elements of which contribute, for example, 38 cm^{-1} for the ground state of H_2 and 27 cm^{-1} for the $B \ ^1\Sigma_u^+$ excited state of H_2 (Bunker, 1968), is neglected here.

To solve Eq. (3.1.1), it would be useful to write the total energy as a sum of contributions from interactions between different particles. In decreasing order of importance, there are: electronic energy, E^{el} , vibrational energy, $G(v)$, and rotational energy, $F(J)$. In fact, this separation is assumed whenever the expression

$$E_{app}^T = E^{el} + G(v) + F(J) \quad (3.1.4)$$

is used to represent observed energy levels. However, Eq. (3.1.4) is always an approximation. It is never possible to express E^T exactly as in Eq. (3.1.4). This means that it is not possible to separate \mathbf{H} rigorously into terms corresponding to the different motions of the particles. The approximate wavefunction suggested by the desired but approximate energy expression, (Eq. (3.1.4)), is a product of two functions,

$$\psi_{i,v}^{BO} = \Phi_{i,\Lambda,S,\Sigma}(r; R) \chi_v(R, \theta, \phi), \quad (3.1.5)$$

where the first factor is the electronic wavefunction and the second is the vibration-rotation wavefunction. Λ is the projection of the electronic orbital angular momentum on the internuclear axis, S is the spin angular momentum, and Σ is its projection on the internuclear axis. The approximate solution [Eq. (3.1.5)] is called a Born-Oppenheimer (BO) product function. It corresponds to a solution where all of the couplings in \mathbf{H} between nuclear and electronic motions are ignored.

3.1.1 Potential Energy Curves

Since \mathbf{T}^N is smaller than \mathbf{T}^e by the factor m/μ , it can be neglected initially. Φ is then the solution of the clamped nuclei electronic Schrödinger equation,

$$[\mathbf{T}^e(r) + V(r, R)]\Phi_i(r; R) = E_i^{el}(R)\Phi_i(r; R) \quad (3.1.6)$$

or

$$\mathbf{H}^{el}\Phi_i = E_i^{el}\Phi_i.$$

If the approximate product function, $\Phi_i\chi$, is inserted into Eq. (3.1.1), after multiplying by Φ_i^* and integrating over the electronic coordinates r , one obtains

$$\langle \Phi_i | \mathbf{T}^N + \mathbf{T}^e + V | \Phi_i \rangle_r \chi = E^T \langle \Phi_i | \Phi_i \rangle_r \chi.$$

The electronic wavefunction is normalized to unity because it is a probability distribution function, $\langle \Phi_i | \Phi_i \rangle_r = 1$. If the effect of $\partial/\partial R$ [contained in $\mathbf{T}^N(R)$] on the electronic wavefunction, which certainly depends on R , is neglected, then

$$\langle \Phi_i | \mathbf{T}^N | \Phi_i \rangle_r \chi \simeq \mathbf{T}^N \langle \Phi_i | \Phi_i \rangle_r \chi = \mathbf{T}^N \chi.$$

Thus, Eq. (3.1.6) may be simplified to

$$\langle \Phi_i | \mathbf{T}^e + V | \Phi_i \rangle_r = E_i^{el}(R),$$

and the result used to obtain the nuclear Schrödinger equation,

$$[\mathbf{T}^N(R, \theta, \phi) + E_i^{el}(R)]\chi(R, \theta, \phi) = E^T \chi(R, \theta, \phi).$$

Since $\mathbf{T}^N(R, \theta, \phi) = \mathbf{T}^N(R) + \mathbf{H}^{\text{ROT}}$, the radial and angular variables can be separated, as in the case of the hydrogen atom (Pauling and Wilson, 1935), as

$$\chi(R, \theta, \phi) = \chi_{v,J}(R) \mathcal{D}_{\Omega M}^J(\alpha = \pi/2, \beta = \theta, \gamma = \phi) = \chi_{v,J}(R) \langle \alpha \beta \gamma | JM \Omega \rangle,$$

where $\langle \alpha \beta \gamma | JM \Omega \rangle$ is the symmetric rotor function defined by Eq. (2.3.41) and $\chi_{v,J}$ is a vibrational eigenfunction of

$$[\mathbf{T}^N(R) + (\hbar^2/2\mu R^2)[J(J+1) - \Omega^2] + E_i^{el}(R)] \chi_{v,J}(R) = E^T \chi_{v,J}(R), \quad (3.1.7)$$

where $\Omega = \Lambda + \Sigma$.

E_i^{el} may be viewed as the potential energy curve in which the nuclei move, but it must be emphasized that potential energy curves do not correspond to any physical observable. They are a concept, derived from a specified set of assumptions for defining a particular type of approximate wavefunctions [Eq. (3.1.5)]. The observed levels are not exact energy eigenvalues of a given potential curve. In general, the separation between the electronic and nuclear motions, which constitutes the BO approximation, is convenient. But when the observed levels do not fit formulas such as Eq. (3.1.4), it is simply because the function [Eq. (3.1.5)] is a bad approximation in that particular case.

An exact solution, ψ_i^T , of the total Hamiltonian \mathbf{H} must satisfy two conditions:

$$\begin{aligned} (i) \quad & \langle \psi_i^T | \mathbf{H} | \psi_i^T \rangle = E_i^T \\ (ii) \quad & \langle \psi_j^T | \mathbf{H} | \psi_i^T \rangle = 0, \quad \text{for any } j \neq i. \end{aligned} \quad (3.1.8)$$

One then says that the Hamiltonian is diagonalized in the basis set $\{\psi^T\}$.

In principle, it is possible to express any exact solution as an infinite expansion over the BO product functions,

$$\psi_i^T = \sum_{j,v_j} c_{i,v_j} \Phi_j^{BO} \chi_{v_j}. \quad (3.1.9)$$

The coefficients of this expansion are determined by diagonalizing a matrix representation of the total Hamiltonian, constructed by evaluating matrix elements between BO basis functions.

It is most useful to define a basis set of the type of Eq. (3.1.5) for which the off-diagonal matrix elements of the total Hamiltonian are as small as possible. If *one term* of the expansion in Eq. (3.1.9) is sufficient, this means that the BO approximation is valid. Fortunately, when the BO approximation fails, often *only two terms* of the BO expansion are sufficient.

If large off-diagonal matrix elements of the Hamiltonian exist that couple *many* vibrational wavefunctions belonging to two different electronic states, then

it is much more convenient to write and solve the coupled differential equations that describe these two states (see Section 4.4.3). The BO approximation fails whenever off-diagonal elements of \mathbf{H} , H_{ij} , connecting different eigenstates of the Eq. (3.1.5) form, are large compared to the difference between the diagonal elements, $H_{ii} - H_{jj}$.

3.1.2 Terms Neglected in the Born-Oppenheimer Approximation

This section deals with various types of nonzero off-diagonal matrix elements of \mathbf{H} between approximate BO product basis functions. *In order to go beyond the BO approximation, to try to obtain an exact solution, it is necessary to use a BO representation.* In other words, the exact eigenvalues and eigenfunctions, which can be compared to observed energy levels, are expressed in terms of the BO representation, specifically as a linear combination of BO product functions.[†] Presently, $\{\psi^{BO}\}$ is the only available type of complete, rigorously definable basis set.

In the following, the off-diagonal matrix elements of

$$\mathbf{H} = \mathbf{H}^{\text{el}} + \mathbf{T}^N(R) + \mathbf{H}^{\text{ROT}}$$

of the form

$$\left\langle \Phi_{i,\Lambda,S,\Sigma} \chi_{v_i,J} | \mathbf{H} | \Phi_{j,\Lambda',S',\Sigma'} \chi_{v'_j,J} \right\rangle$$

will be discussed. The off-diagonal matrix elements of \mathbf{H}^{el} give rise to *electrostatic perturbations*. The off-diagonal matrix elements of $\mathbf{T}^N(R)$ give rise to *nonadiabatic interactions*. The off-diagonal matrix elements of \mathbf{H}^{ROT} give rise to *rotational perturbations*. The total Hamiltonian discussed above does not include the relativistic part of the Hamiltonian. That contribution to \mathbf{H} will be introduced as a phenomenological perturbation operator, \mathbf{H}^{SO} , and will give rise to *spin-orbit perturbations*.

3.1.2.1 Electrostatic and Nonadiabatic Part of \mathbf{H}

In Section 3.3 it will be shown that, to describe perturbations which result from neglected terms in the $\mathbf{H}^{\text{el}} + \mathbf{T}^N(R)$ part of the Hamiltonian, two different types of BO representations are useful. If a crossing (diabatic) potential curve representation is used, off-diagonal matrix elements of \mathbf{H}^{el} appear between the states of this representation. If a noncrossing (adiabatic) potential curve representation is the starting point, the \mathbf{T}^N operator becomes responsible for perturbations.

[†] It is *never* appropriate to take linear combinations of vibrational basis states which belong to different potential curves unless the associated electronic and rotational factors are included.

3.1.2.1.1 Crossing or Diabatic Curves

If Φ_i and Φ_j are two different exact solutions of Eq. (3.1.6), then

$$\langle \Phi_i | \mathbf{H}^{\text{el}} | \Phi_j \rangle = 0$$

It will be shown later that *exact* solutions of the electronic Schrödinger equation can give rise to double minimum potential curves. Such potentials can be inconvenient for treating some perturbation situations. It is often more convenient to start from *approximate* solutions of \mathbf{H}^{el} where potential curves, which would have avoided crossing for the exact \mathbf{H}^{el} , actually cross. In such a case,

$$\langle \Phi_i^{\text{app}} | \mathbf{H}^{\text{el}} | \Phi_j^{\text{app}} \rangle_r = H_{i,j}^e(R) \neq 0. \quad (3.1.10)$$

The expression for \mathbf{H}^{el} includes $\mathbf{T}^e(r)$ [Eq. (3.1.3c)] and $V(r, R)$, where

$$V(r, R) = V^{eN}(r, R) + V^{ee}(r) + V^{NN}(R);$$

$V^{eN}(r, R)$ is the Coulomb electron-nuclear attraction energy operator,

$$V^{eN}(r, R) = - \sum_{i=1}^n \left(\frac{Z_A e^2}{r_{Ai}} + \frac{Z_B e^2}{r_{Bi}} \right);$$

$V^{ee}(r)$ is the Coulomb interelectronic repulsion energy operator,

$$V^{ee}(r) = \sum_{i=1}^n \sum_{j>i} \frac{e^2}{r_{ij}},$$

where $j > i$ ensures that each repulsion between the i th and j th electrons is considered only once; and $V^{NN}(R)$ is the Coulomb internuclear repulsion energy operator,

$$V^{NN}(R) = Z_A Z_B e^2 / R.$$

Note that the negative sign of V^{eN} implies that it contributes to energy stabilization. Crossing curves are obtained by excluding parts of the spin-orbit term, \mathbf{H}^{SO} , and of the interelectronic term, V^{ee} , from the \mathbf{H}^{el} operator.[†] The effect of V^{ee} , discussed in Section 3.3.2, is extremely important as it compromises the validity of the *single electronic configuration* picture which is often taken as synonymous with the diabatic potential curve picture.

In both crossing and noncrossing curve approaches, perturbations between levels of the same symmetry can occur. In the diabatic picture, these are usually called “electrostatic perturbations” because they arise from V^{ee} . In the adiabatic picture, they arise from \mathbf{T}^N , the nuclear kinetic energy operator, but are often misleadingly called electrostatic perturbations.

[†] It is not possible to give a unique definition of a diabatic potential curve without identifying the specific term in \mathbf{H}^{el} that is excluded. The impossibility of identifying such a term and the consequent nonuniqueness of the *a priori* definition of diabatic curves is discussed by Lewis and Hougen (1968), Smith (1969), and Mead and Truhlar (1982) (See also Section 3.3.2). Diabatic curves may be defined empirically (Section 3.3) by assuming a deperturbation model [e.g., that $H_{i,j}^e(R)$ is independent of R or, at most, varies linearly with R].

3.1.2.1.2 Noncrossing or Adiabatic Curves

Equation (3.1.7) was obtained by assuming that $\mathbf{T}^N(R)$ does not act on the electronic wavefunction. Actually, the Φ_i are functions of the nuclear coordinate, R . Adding to Eq. (3.1.7) the neglected R -dependent term

$$\langle \Phi_i | \mathbf{T}^N | \Phi_i \rangle_r,$$

where integration over all electronic coordinates and the θ, ϕ nuclear coordinates is implied, one obtains

$$\begin{aligned} & [\mathbf{T}^N(R) + (\hbar^2/2\mu R^2)[J(J+1) - \Omega^2] + \langle \Phi_i | \mathbf{T}^N | \Phi_i \rangle_r + E_i^{el}(R)] \chi_{v,J}(R) \\ & = E^T \chi_{v,J}(R). \end{aligned} \quad (3.1.11)$$

The potential curves defined by

$$E_i^{ad}(R) = E_i^{el}(R) + \langle \Phi_i | \mathbf{T}^N | \Phi_i \rangle_r$$

are called adiabatic potential curves, but the second term makes a much smaller contribution to the energy than $E^{el}(R)$ (Bunker, 1968).

The off-diagonal matrix element $\langle \Phi_i | \mathbf{T}^N | \Phi_j \rangle_r$, the nonadiabatic coupling term, is examined in Section 3.3.3. This type of matrix element appears between states of identical symmetry and gives rise to homogeneous perturbations.

3.1.2.2 The Spin Part of \mathbf{H}

Equation (3.1.2) is the nonrelativistic Hamiltonian. This means that the spin-dependent part of the Hamiltonian (\mathbf{H}^{SO} spin-orbit and \mathbf{H}^{SS} spin-spin) has been neglected. The electronic angular momentum quantum numbers, which are well-defined for eigenfunctions of nonrelativistic adiabatic and diabatic potential curves, are Λ , Σ , and S (and redundantly, $\Omega = \Lambda + \Sigma$).

Off-diagonal matrix elements,

$$\langle \Phi_{i,\Lambda,\Sigma,\Omega} | \mathbf{H}^{\text{SO}} + \mathbf{H}^{\text{SS}} | \Phi_{j,\Lambda',\Sigma',\Omega} \rangle,$$

can be nonzero between states of different Λ and S (but identical Ω) quantum numbers, corresponding to different solutions [Eq. (3.1.5)] of the nonrelativistic Hamiltonian [Eq. (3.1.2)]. Matrix elements of this type are discussed in Section 3.4. The spin-spin part, \mathbf{H}^{SS} , of the spin Hamiltonian usually gives rise to matrix elements much smaller than those of \mathbf{H}^{SO} and \mathbf{H}^{el} .

The relativistic Hamiltonian may be defined by adding \mathbf{H}^{SO} to \mathbf{H}^{el} . The eigenfunctions of this new Hamiltonian are the relativistic wavefunctions, $\Phi_{i,\Omega}$, which define the relativistic potential curves

$$\langle \Phi_{i,\Omega} | \{ \mathbf{H}^{el}(R) + \mathbf{H}^{\text{SO}}(R) \} | \Phi_{i,\Omega} \rangle_r = E_i^r(R), \quad (3.1.12)$$

where now the only good electronic angular momentum quantum number is $\Omega = \Lambda + \Sigma$.

Table 3.1 summarizes the different types of potential energy curves and the specific terms in \mathbf{H} that are neglected in order to define the diabatic, adiabatic, relativistic-adiabatic, and relativistic-diabatic basis functions.

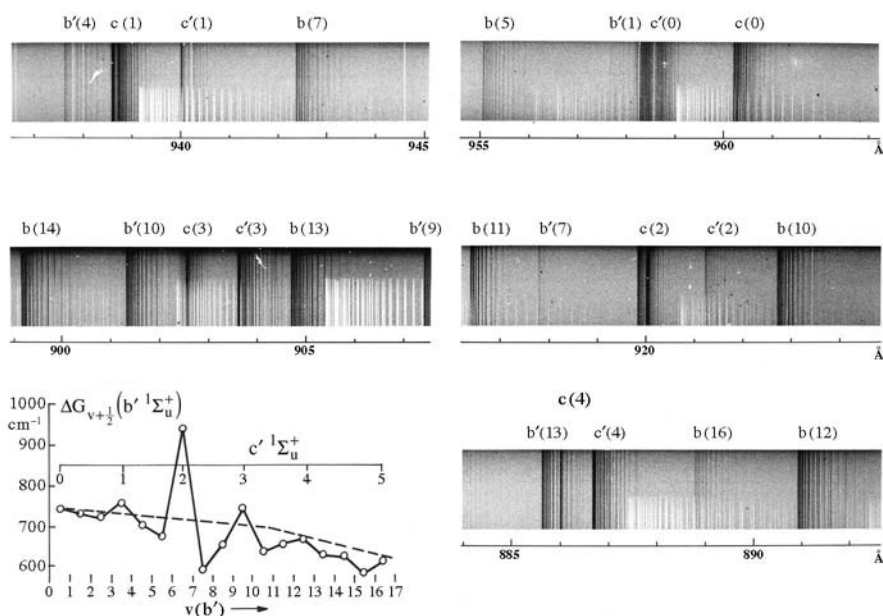


Figure 3.4: Electrostatic valence~Rydberg N_2 $b'^1\Sigma_u^+(v_{b'}) \sim c'^1\Sigma_u^+(v_{c'})$ and $b^1\Pi_u(v_b) \sim c^1\Pi_u(v_c)$ perturbations. Each segment of the absorption spectrum (from Yoshino, *et al.*, 1979) shows several perturbing states near a nominal $v_{c'} = 0 - 4$ $c'^1\Sigma_u^+$ level. The b and b' valence states are perturbed by the c and c' Rydberg states (nominally the $^1\Pi_u$ and $^1\Sigma_u^+$ components of a $3p$ complex) as well as by higher Rydberg states. The $\Delta G_{v+1/2}$ plot for the $b'^1\Sigma_u^+$ state (from Dressler, 1969; see also Fig. 3.6) in the lower left corner shows the massive level shifts that had made it difficult to recognize the electronic state parentage of the observed singlet vibronic levels of N_2 . The largest positive deviations of the observed ΔG values from the smoothly varying deperturbed value (dashed line) occur when the $v_{b'} = 1, 2$ and 3 levels are sandwiched between the $v_{b'} = 3$ and $4, 6$ and $7, 9$ and 10 levels, respectively. These $b' \sim c'$ perturbations are discussed in Section 6.3.1 and further illustrated in Fig. 3.6.

but then

$$\langle \Phi_1^{ad} | \mathbf{T}^N | \Phi_2^{ad} \rangle_r \neq 0. \quad (3.3.3)$$

In principle, whatever the initial model, after introducing the vibronic coupling terms corresponding to the chosen type of deperturbed potential curves, the experimental energy levels are obtained by diagonalizing one or the other type of interaction matrix. One example will be discussed later (Section 3.3.4).

If the deperturbed curves intersect and are characterized by very different molecular constants, then they are diabatic curves (see Fig. 3.5). If the crossing is avoided, adiabatic curves are involved, and one of these curves can have a double minimum. One frequently finds that, in the region of an avoided crossing, the adiabatic wavefunction changes electronic character abruptly and the derivative of the electronic wavefunction with respect to R can be large. In

fact, it is this derivative that controls the size of the matrix elements of the \mathbf{T}^N operator [Eq. (3.3.10)].

In the older literature (Dieke, 1935; Kovács, 1969), there is some confusion. Only the \mathbf{T}^N operator has been assumed to connect states of the same symmetry, and the potential curves of these interacting states have been assumed to cross. Neither assumption is correct.

3.3.1 Diabatic Curves

The vibronic interaction between the level v_1 of the diabatic potential curve $V_1^d(R)$ and the level v_2 of another diabatic curve $V_2^d(R)$ is reduced to

$$H_{1,v_1;2,v_2} = \langle \Phi_1^d \chi_{v_1}^d | \mathbf{H}^{\text{el}} | \Phi_2^d \chi_{v_2}^d \rangle \quad (3.3.4)$$

since, by definition,

$$\langle \Phi_1^d | \mathbf{T}^N | \Phi_2^d \rangle = 0.$$

In the diabatic model, the electronic part of the matrix element $H_{1,v_1;2,v_2}$ is often assumed to be independent of R . Then the nuclear and electronic coordinates can be separated in the integration of Eq. (3.3.4). By integration over the electronic coordinates, one obtains

$$H_{1,v_1;2,v_2} = H^e \langle v_1^d | v_2^d \rangle, \quad (3.3.5)$$

where

$$H^e = \langle \Phi_1^d | \mathbf{H}^{\text{el}} | \Phi_2^d \rangle$$

and

$$\langle v_1^d | v_2^d \rangle = \int \chi_{v_1}^{d*}(R) \chi_{v_2}^d(R) dR.$$

Indeed, as for any electronic quantity, the value of H^e actually depends on R . However, this dependence is usually weak. Equation (3.3.5) holds even if the R -dependence of H^e is a linear function of the R -centroid (Halevi, 1965) defined by

$$\bar{R}_{ij} = \frac{\langle v_i | R | v_j \rangle}{\langle v_i | v_j \rangle}. \quad (3.3.6a)$$

The significance of the R -centroid is illustrated as follows. The electronic matrix element, $H^e(R)$, may be expanded in a power series about an arbitrarily chosen internuclear distance, R' (most usefully, $R' = R_C$, the internuclear distance at which the two potential curves cross),

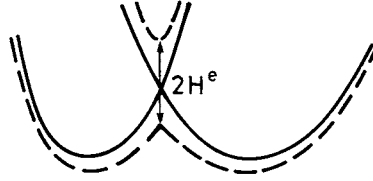


Figure 3.5: Diabatic and adiabatic potential curves. The diabatic curves (solid lines) cross at R_c and are defined by neglecting the part of \mathbf{H}^{el} that causes the adiabatic curves (dotted lines) to avoid crossing by $2H^e$ at R_c .

$$H^e(R) = H^e(R') + \left(\frac{dH^e}{dR} \right)_{R=R'} (R - R') + \frac{1}{2} \left(\frac{d^2H^e}{dR^2} \right)_{R=R'} (R - R')^2. \quad (3.3.7a)$$

Then the vibrational matrix elements of $H^e(R)$ are expressed in terms of R^n -centroids,

$$\overline{R}_{ij}^n = \frac{\langle v_i | R^n | v_j \rangle}{\langle v_i | v_j \rangle} \quad (3.3.6b)$$

$$\begin{aligned} \langle v_i | H^e(R) | v_j \rangle &= H^e(R') \langle v_i | v_j \rangle + \left(\frac{dH^e}{dR} \right)_{R=R'} [\langle v_i | R | v_j \rangle - R' \langle v_i | v_j \rangle] \\ &\quad + \frac{1}{2} \left(\frac{d^2H^e}{dR^2} \right)_{R=R'} [\langle v_i | R^2 | v_j \rangle - 2R' \langle v_i | R | v_j \rangle + R'^2 \langle v_i | v_j \rangle] \end{aligned}$$

$$\begin{aligned} \frac{\langle v_i | H^e(R) | v_j \rangle}{\langle v_i | v_j \rangle} &= H^e(R') + \left(\frac{dH^e}{dR} \right)_{R=R'} [\overline{R}_{ij} - R'] \\ &\quad + \frac{1}{2} \left(\frac{d^2H^e}{dR^2} \right)_{R=R'} [\overline{R}_{ij}^2 - 2R' \overline{R}_{ij} + R'^2]. \quad (3.3.7b) \end{aligned}$$

Now, making the R -centroid *approximation*, which is quite distinct from the R^n -centroid expansion, namely,

$$\bar{R} \simeq \frac{\overline{R}_{ij}^n}{\overline{R}_{ij}^{n-1}} = \frac{\langle v_i | R^n | v_j \rangle}{\langle v_i | R^{n-1} | v_j \rangle}$$

[or, in other words, $\overline{R}^n = (\bar{R})^n$], then Eq. (3.3.7b) becomes

$$\begin{aligned} \frac{\langle v_i | H^e(R) | v_j \rangle}{\langle v_i | v_j \rangle} &= H^e(R') + \left(\frac{dH^e}{dR} \right)_{R=R'} (\bar{R}_{ij} - R') \\ &\quad + \frac{1}{2} \left(\frac{d^2H^e}{dR^2} \right)_{R=R'} (\bar{R}_{ij} - R')^2, \end{aligned}$$

which is identical to Eq. (3.3.7a) where R is set equal to \overline{R}_{ij} .

For near-degenerate vibrational levels of any two crossing potential curves, the R -centroid has the convenient property of being nearly equal to R_C , the R -value where the two curves cross (Schamps, 1977). Thus,

$$\overline{R} = \overline{R^k} / \overline{R^{k-1}} = R_C,$$

and, setting $R' = R_C$,

$$\frac{\langle v_i | H^e | v_j \rangle}{\langle v_i | v_j \rangle} = H^e(R_C).$$

The R -centroid approximation has repeatedly been tested numerically. For perturbations between levels of potentials that intersect exactly once, the R -centroid approximation can be regarded as more accurate than experimentally measurable matrix elements.

The validity of the R -centroid approximation is based on a stationary phase argument (see Section 5.1.1) (Tellinghuisen 1984). For two vibrational states, $|v_i\rangle$ and $|v_j\rangle$, at nearly identical total energy, the vibrational overlap integral

$$I(R') = \int_0^{R'} \langle v_i | R \rangle \langle R | v_j \rangle dR$$

accumulates only near $R' = R_C$, where the two vibrational wavefunctions oscillate at the same spatial frequency. This stationary phase argument works equally well at low and high v and for R_C near or far from vibrational turning points, provided that there is only one intersection between the potential curves within the range of R defined by the vibrational turning points at the total energy of the perturbation.

Approximate deperturbed curves can be derived from unperturbed vibrational levels far from the energy of the curve crossing region. The overlap factor between vibrational wavefunctions is calculable numerically. (Note that a Franck-Condon factor is the absolute magnitude squared of the overlap factor.) From Eq. (3.3.5) and the experimental value of $H_{1,v_1;2,v_2}$, an initial trial value for H^e can be deduced. If the value of H^e is as large as the value of ω_e (see Table 4.4), then electrostatic interactions strongly perturb the entire set of vibrational levels. Figure 3.6 shows the irregular pattern of ΔG values for the perturbed ${}^1\Sigma_u^+$ states of N_2 . Final deperturbed curves are obtained by diagonalization of the matrix, including all vibrational levels of both states, as described in Section 4.4.

3.3.2 Approximate Representation of the Diabatic Electronic Wavefunction

The single-configuration approximation is an approximate representation for the diabatic electronic function. Such an approximation is expected to result in

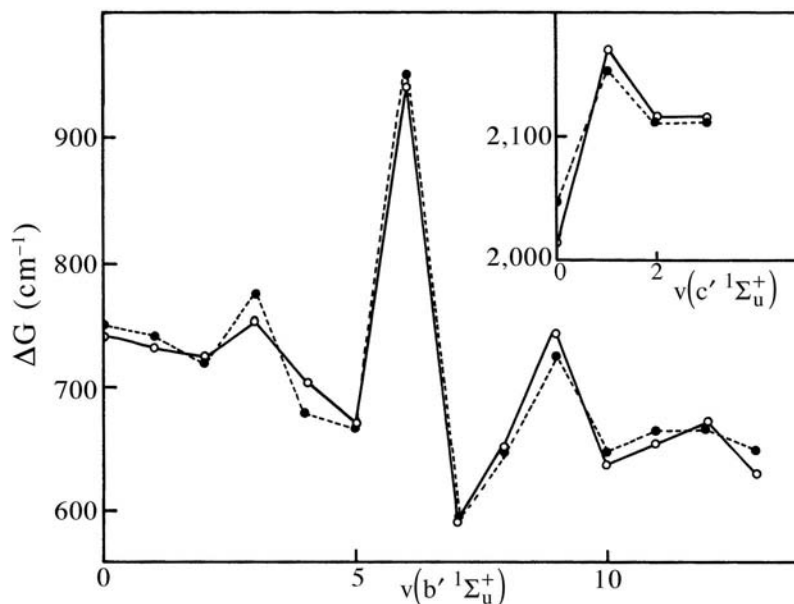


Figure 3.6: Variation of ΔG_v for the mutually interacting b' and $c'{}^1\Sigma_u^+$ states of N_2 . The solid and dashed lines correspond, respectively, to the observed and calculated (Lefebvre-Brion, 1969) values. The deperturbed c' ($v = 2$) and b' ($v = 7$) levels are nearly degenerate and interact strongly (see Table 5.4). This accounts for the largest ΔG anomalies.

smooth R -variation of the electronic wavefunction. In the case where the configurations of the two interacting states differ by two spin-orbitals, the electronic matrix element of the \mathbf{T}^N operator between these two approximate functions is exactly zero, since it can be demonstrated that the \mathbf{T}^N operator acts as a one-electron operator (Section 3.2.4) (Sidis and Lefebvre-Brion, 1971). However, as the electronic Hamiltonian, \mathbf{H}^{el} , contains a two-electron operator,

$$\sum_{i < j} \frac{e^2}{r_{ij}},$$

\mathbf{H}^{el} can have nonzero matrix elements. If the unique orbitals are ϕ_a, ϕ_b and ϕ_c, ϕ_d for the two electronic configurations, then Eq. (3.2.54) and Eq. (3.2.55) give

$$H^e \propto \langle \phi_a \phi_c | 1/r_{12} | \phi_b \phi_d \rangle - \langle \phi_a \phi_d | 1/r_{12} | \phi_b \phi_c \rangle. \quad (3.3.8)$$

If the spin parts of ϕ_a and ϕ_b are identical, both terms in Eq. (3.3.8) are nonzero. Otherwise, the single nonzero term is the one in which the spins of electron 1 and those of electron 2 are identical (i.e., $\langle \phi_a \phi_c | 1/r_{12} | \phi_b \phi_d \rangle = 0$

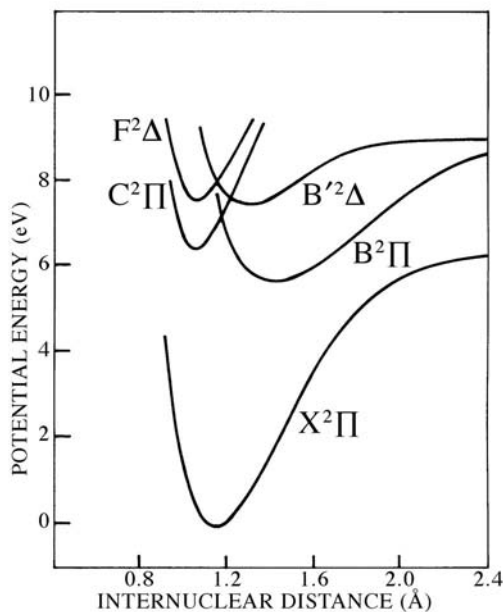


Figure 3.7: ${}^2\Delta$ and ${}^2\Pi$ potential energy curves of NO. The $C^2\Pi$ Rydberg state is homogeneously perturbed by the $B^2\Pi$ valence state. Similarly, the $F^2\Delta$ Rydberg state is perturbed by the $B'^2\Delta$ valence state.

unless the spin parts of ϕ_a and ϕ_b , respectively, match those of ϕ_c and ϕ_d). In the case where the two configurations differ by only one *orbital*, but still by two *spin-orbitals*, more complicated formulas apply[†]. This situation would occur for two Rydberg states of the same symmetry that belong to series converging to ion-core states of different multiplicities (see Section 5.2.4 for an example of ${}^3\Sigma_u^-$ Rydberg states belonging to series converging to ${}^2\Sigma_g^-$ and ${}^4\Sigma_g^-$ ion cores).

It will be shown in Section 5.2 that electrostatic perturbations occur frequently between states whose configurations differ by two orbitals, especially between Rydberg and valence states. An example from the NO spectrum is discussed here (Fig. 3.7). The $B'^2\Delta$ valence state of the NO molecule can be represented by the configuration $\sigma 2p \pi 2p^4 \pi^* 2p^2$. The $F^2\Delta$ state belongs to a Rydberg series that converges to the ground state of the NO^+ ion and is represented by the $\sigma 2p^2 \pi 2p^4 3d\delta$ configuration. The configurations of the $B'^2\Delta$ and $F^2\Delta$ states differ by two orbitals that have different spin functions. The electrostatic interaction is given by

$$H^e = \langle \sigma 2p \pi^* 2p | 1/r_{12} | 3d\delta \pi^* 2p \rangle.$$

[†]The added complication arises from the necessity to express the wavefunctions for states with multiple open subshells as properly symmetrized sums of Slater determinantal functions. H^e will then include off-diagonal matrix elements between several pairs of Slater determinants.

This integral has been evaluated *ab initio* and found equal to 300 cm^{-1} (Felenbok and Lefebvre-Brion, 1966). (The one-center part of this integral is approximately the nonzero atomic integral $\langle sp | 1/r_{12} | dp \rangle$.) This calculated value is in fair agreement with the “semiexperimental” value of 450 cm^{-1} found by a de-perturbation procedure (Jungen, 1966). Note that this electrostatic interaction is responsible not only for perturbations between states of identical symmetry but also for predissociation (Section 7.8.1) and auto-ionization (Section 8.8).

Owing to numerical difficulties associated with minimizing the radial ($\partial/\partial R$ and $\partial^2/\partial R^2$) couplings, other ways to theoretically calculate diabatic states have been proposed (Yarkony, 2000; Köppel, *et al.*, 1984). Since, in the region of the avoided crossing, some characteristics of the wavefunctions are interchanged, several molecular properties will reflect this change. Consequently, diabatic states can be defined by requiring the smoothness of the R -dependence of a molecular property such as the dipole moment or electronic transition moment. The transformation matrix between the diabatic and adiabatic states can be obtained by diagonalizing the adiabatic dipole (Weiner and Meyer, 1981) or quadrupole (Li, *et al.*, 1997) moment matrix.

3.3.3 Adiabatic Curves

In the adiabatic model, the matrix element between the v_1 level of the first adiabatic curve $V_1^{ad}(R)$ and the v_2 level of the second adiabatic curve $V_2^{ad}(R)$ (see Fig. 3.5) is reduced to

$$H_{1,v_1;2,v_2} = \langle \Phi_1^{ad} \chi_{v_1}^{ad} | \mathbf{T}^N | \Phi_2^{ad} \chi_{v_2}^{ad} \rangle, \quad (3.3.9)$$

and

$$\langle \Phi_1^{ad} | \mathbf{H}^{\text{el}} | \Phi_2^{ad} \rangle = 0.$$

\mathbf{T}^N is the nuclear kinetic energy operator, which is expressed in the molecular frame as

$$\mathbf{T}^N = -\frac{\hbar^2}{2\mu R^2} \left\{ \frac{\partial}{\partial R} \left[R^2 \frac{\partial}{\partial R} \right] - \mathbf{R}^2 \right\} = -\frac{\hbar^2}{2\mu} \left[\frac{\partial^2}{\partial R^2} + \frac{2}{R} \frac{\partial}{\partial R} \right] + \frac{\hbar^2}{2\mu R^2} \mathbf{R}^2.^\dagger$$

Let us ignore the \mathbf{R}^2 rotational part ($\mathbf{R}=\mathbf{J}-\mathbf{L}-\mathbf{S}$) of this operator, which leads to off-diagonal matrix elements that are proportional to $J(J+1)$ but still very small compared to the matrix elements of the remaining radial term (Leoni, 1972). The effect of the derivatives with respect to R on the electronic and vibrational wavefunctions, both of which depend on R , is given by

$$\frac{\partial^2(\Phi\chi)}{\partial R^2} = \chi \frac{\partial^2\Phi}{\partial R^2} + \Phi \frac{d^2\chi}{dR^2} + 2 \frac{\partial\Phi}{\partial R} \frac{d\chi}{dR}$$

[†] Recall that R is the internuclear distance and \mathbf{R} is the nuclear rotation angular momentum.

and

$$\frac{2}{R} \frac{\partial}{\partial R} \Phi \chi = \frac{2}{R} \chi \frac{\partial \Phi}{\partial R} + \frac{2}{R} \Phi \frac{d\chi}{dR}.$$

Combining this result with Eq. (3.3.9) yields

$$\begin{aligned} H_{1,v_1;2,v_2} = & -\frac{\hbar^2}{2\mu} \left\langle \chi_{v_1}^{ad} \left| \left\langle \Phi_1^{ad} \left| \frac{\partial^2}{\partial R^2} + \frac{2}{R} \frac{\partial}{\partial R} \right| \Phi_2^{ad} \right\rangle_r \right| \chi_{v_2}^{ad} \right\rangle_R \\ & -\frac{\hbar^2}{2\mu} \left\langle \Phi_1^{ad} | \Phi_2^{ad} \right\rangle_r \left\langle \chi_{v_1}^{ad} \left| \frac{d^2}{dR^2} + \frac{2}{R} \frac{d}{dR} \right| \chi_{v_2}^{ad} \right\rangle_R \\ & -\frac{\hbar^2}{\mu} \left\langle \chi_{v_1}^{ad} \left| \left\langle \Phi_1^{ad} \left| \frac{\partial}{\partial R} \right| \Phi_2^{ad} \right\rangle_r \right| \frac{d}{dR} \chi_{v_2}^{ad} \right\rangle_R. \end{aligned} \quad (3.3.10)$$

In Eq. (3.3.10), the second term is zero after integration over the electronic coordinates r , since Φ_1^{ad} and Φ_2^{ad} are two different solutions of the same equation and must therefore be orthogonal. The off-diagonal matrix elements in Eq. (3.3.10) are often called nonadiabatic corrections to the energies.

The vibrational wavefunction is often written as $\chi = \xi/R$, where ξ is normalized with respect to dR (as opposed to $R^2 dR$ as for χ). Then the derivative of the vibrational function with respect to R results in two terms. One of these terms exactly cancels the term in $(2/R)(\partial\Phi/\partial R)$ of Eq. (3.3.10), and the matrix element simplifies to

$$\begin{aligned} H_{1,v_1;2,v_2}(\text{cm}^{-1}) = & \frac{-16.8576}{\mu(\text{amu})} \left\langle \xi_{v_1}^{ad} \left| \left\langle \Phi_1^{ad} \left| \frac{\partial^2}{\partial R^2} \right| \Phi_2^{ad} \right\rangle_r (\text{\AA}^{-2}) \right| \xi_{v_2}^{ad} \right\rangle_R \\ & -\frac{33.7152}{\mu(\text{amu})} \left\langle \xi_{v_1}^{ad} \left| \left\langle \Phi_1^{ad} \left| \frac{\partial}{\partial R} \right| \Phi_2^{ad} \right\rangle_r (\text{\AA}^{-1}) \right| \frac{d}{dR} \xi_{v_2}^{ad} \right\rangle_R (\text{\AA}^{-1}). \end{aligned} \quad (3.3.11)$$

In the case where an avoided crossing is being represented by adiabatic curves, a relation between electronic matrix elements for basis functions belonging to adiabatic versus diabatic curves can be derived easily (Bandrauk and Child, 1970; Oppenheimer, 1972), as shown below.

Adiabatic potential curves can be obtained by diagonalizing, at a grid of R -values, the configuration-interaction matrix. This matrix is constructed in a particular diabatic (single-configuration) basis. The off-diagonal configuration-interaction matrix element is the familiar diabatic coupling term, $H_{12}^e(R)$, which involves integration over electronic coordinates at a fixed value of internuclear distance [Eq. (3.1.10)]. The configuration-interaction secular equation is

$$\begin{vmatrix} E_1^d(R) - E & H_{12}^e(R) \\ H_{12}^e(R) & E_2^d(R) - E \end{vmatrix} = 0 \quad (3.3.12)$$

where $E_i^d(R)$ is defined by the fixed- R integral over electronic coordinates,

$$E_i^d(R) = \left\langle \Phi_i^d | \mathbf{H}^{\text{el}} | \Phi_i^d \right\rangle_r.$$

The resultant eigenstates are found to be linear combinations of diabatic electronic functions, for which the configuration interaction mixing coefficients are explicitly dependent on internuclear distance,

$$\begin{aligned}\Phi_1^{ad} &= \cos\theta(R)\Phi_1^d - \sin\theta(R)\Phi_2^d, \\ \Phi_2^{ad} &= \sin\theta(R)\Phi_1^d + \cos\theta(R)\Phi_2^d.\end{aligned}\tag{3.3.13}$$

These expressions imply that the functions Φ_i^{ad} are orthogonal. At the crossing point $R = R_C, \theta = \pi/4$.

The vertical energy separation between two interacting diabatic potentials can be assumed to vary linearly with R in the crossing region,

$$E_1^d(R) - E_2^d(R) = a(R - R_C).$$

Now, as the Φ_i^d functions are diabatic, the derivative with respect to R acts only on the coefficients of the linear combinations in Eq. (3.3.13), thus

$$\left\langle \Phi_1^{ad} \left| \frac{\partial}{\partial R} \right| \Phi_2^{ad} \right\rangle_r = [\sin^2\theta + \cos^2\theta] \frac{\partial\theta}{\partial R} = \frac{\partial\theta}{\partial R}.$$

By definition, the adiabatic functions Φ_1^{ad} and Φ_2^{ad} diagonalize the electronic Hamiltonian. Using Eq. (3.3.13), one finds ($H^e \equiv H_{12}^e$)

$$\begin{aligned}\langle \Phi_1^{ad} | \mathbf{H}^{el} | \Phi_2^{ad} \rangle_r \\ = +E_1^d \sin\theta \cos\theta - H^e \sin^2\theta + H^e \cos^2\theta - E_2^d \sin\theta \cos\theta = 0,\end{aligned}$$

from which the R -dependence of θ near R_C may be determined,

$$\frac{\sin\theta \cos\theta}{\cos^2\theta - \sin^2\theta} = \frac{1}{2} \tan 2\theta = \frac{H^e}{E_2^d - E_1^d} = -\frac{H^e}{a(R - R_C)}.$$

Thus,

$$\theta = \frac{1}{2} \tan^{-1} \left[\frac{-2H^e}{a(R - R_C)} \right] = \frac{1}{2} \cot^{-1} \left[\frac{a(R - R_C)}{-2H^e} \right],$$

and since

$$\frac{d}{dx} \cot^{-1} \left(\frac{x}{c} \right) = \frac{-c}{c^2 + x^2}$$

then

$$\left\langle \Phi_1^{ad} \left| \frac{\partial}{\partial R} \right| \Phi_2^{ad} \right\rangle_r = \frac{\partial\theta}{\partial R} = \frac{aH^e}{4(H^e)^2 + a^2(R - R_C)^2}.$$

Table 3.5: Comparison between Diabatic and Adiabatic Parameters

Interacting States	Molecule	H^e (cm ⁻¹)	Maximum value of $W^e(R)$ (Å ⁻¹)	Width (Å) FWHM of $W^e(R)$
$B^2\Sigma_u^+ \sim C^2\Sigma_u^+$	N_2^{+a}	10,000	3.0	0.34
$E, F^1\Sigma_g^+ \sim G, K^1\Sigma_g^+$	H_2^b	$\sim 3,000$	3.4	0.26
$G^1\Pi \sim I^1\Pi$	SiO^c	~ 400	6.4	0.16
$C^3\Pi_u \sim C'^3\Pi_u$	N_2^d	1,000	~ 20.4	0.05
$B^3\Sigma_u^- \sim B'^3\Sigma_u^-$	O_2^e	4,000	21.6	0.06

^aRoche and Lefebvre-Brion, 1975.

^bDressler, *et al.*, 1979.

^cLagerqvist and Renhorn, 1979 (semiexperimental value).

^dRobbe, 1978.

^eYoshimine and Tanaka, 1978.

Defining $b = H^e/a$, then

$$\left\langle \Phi_1^{ad} \left| \frac{\partial}{\partial R} \right| \Phi_2^{ad} \right\rangle_r = \frac{b}{4b^2 + (R - R_C)^2} = W^e(R). \quad (3.3.14)$$

If the diabatic coupling matrix element, H^e , is R -independent, this $\partial/\partial R$ matrix element between two adiabatic states must have a Lorentzian R -dependence with a full width at half maximum (FWHM) of $4b$. Evidently, the adiabatic electronic matrix element $W^e(R)$ is not R -independent but is strongly peaked near R_C . Its maximum value occurs at $R = R_C$ and is equal to $1/4b = a/4H^e$. Thus, if the diabatic matrix element H^e is large, the maximum value of the electronic matrix element between adiabatic curves is small. This is the situation where it is convenient to work with deperturbed adiabatic curves. On the contrary, if H^e is small, it becomes more convenient to start from diabatic curves. Table 3.5 compares the values of diabatic and adiabatic parameters. The deviation from the relation, $W^e(R)_{\max} \times \text{FWHM} = 1$, is due to a slight dependence of H^e on R and a nonlinear variation of the energy difference between diabatic potentials. When $W^e(R)$ is a relatively broad curve without a prominent maximum, the adiabatic approach is more convenient. When $W^e(R)$ is sharply peaked, the diabatic picture is preferable. The first two cases in Table 3.5 would be more convenient to treat from an adiabatic point of view. The description of the last two cases would be simplest in terms of diabatic curves. The third case is intermediate between the two extreme cases and will be examined later (see Table 3.6).

To obtain the second adiabatic electronic matrix element of Eq. (3.3.11), the ket, $(\partial/\partial R) |\Phi_2^{ad}\rangle$, is expanded using the complete set, $\{\Phi_j^{ad}\}$, of adiabatic

functions

$$\begin{aligned}
\frac{\partial}{\partial R} \left| \Phi_2^{ad} \right\rangle &= \sum_i \left| \Phi_i^{ad} \right\rangle \left\langle \Phi_i^{ad} \left| \frac{\partial}{\partial R} \right| \Phi_2^{ad} \right\rangle \\
\frac{\partial^2}{\partial R^2} \left| \Phi_2^{ad} \right\rangle &= \frac{\partial}{\partial R} \frac{\partial}{\partial R} \left| \Phi_2^{ad} \right\rangle = \sum_i \left\{ \frac{\partial}{\partial R} \left| \Phi_i^{ad} \right\rangle \right\} \left\langle \Phi_i^{ad} \left| \frac{\partial}{\partial R} \right| \Phi_2^{ad} \right\rangle \\
&\quad + \sum_i \left| \Phi_i^{ad} \right\rangle \frac{\partial}{\partial R} \left\langle \Phi_i^{ad} \left| \frac{\partial}{\partial R} \right| \Phi_2^{ad} \right\rangle \\
\left\langle \Phi_1^{ad} \left| \frac{\partial^2}{\partial R^2} \right| \Phi_2^{ad} \right\rangle &= \sum_{i \neq 1,2} \left[\left\langle \Phi_1^{ad} \left| \frac{\partial}{\partial R} \right| \Phi_i^{ad} \right\rangle \left\langle \Phi_i^{ad} \left| \frac{\partial}{\partial R} \right| \Phi_2^{ad} \right\rangle \right. \\
&\quad \left. + \frac{\partial}{\partial R} \left\langle \Phi_1^{ad} \left| \frac{\partial}{\partial R} \right| \Phi_2^{ad} \right\rangle \right].
\end{aligned}$$

The second summation reduces to a single term because the adiabatic functions are orthonormal (Hobey and McLachlan, 1960). In the simple case where only two electronic states interact (Eq. (3.3.13)), one can assume that the matrix elements of $\partial/\partial R$ connecting either of these two states with other states are negligible and, from Eq. (3.3.14),

$$\left\langle \Phi_1^{ad} \left| \frac{\partial^2}{\partial R^2} \right| \Phi_2^{ad} \right\rangle_r = \frac{\partial}{\partial R} \left\langle \Phi_1^{ad} \left| \frac{\partial}{\partial R} \right| \Phi_2^{ad} \right\rangle_r = \frac{\partial}{\partial R} W^e(R).$$

This calculated matrix element of $\partial^2/\partial R^2$, acting on the electronic wavefunctions for the E, F and G, K states of H_2 (Fig. 3.8), is displayed in Fig. 3.9 and is seen not to deviate appreciably from the derivative of a Lorentzian curve. Its contribution to the $H_{1,v_m;2,v_n}$ vibronic matrix element [Eq. (3.3.11)] is generally smaller than the contribution due to the $\partial/\partial R$ operator acting on the electronic functions, but it is in no case negligible.

3.3.4 Choice between the Diabatic and Adiabatic Models

If the approximate deperturbed potential curves cross, they are diabatic curves. One can assume an interaction matrix element given by Eq. (3.3.5) and carry out a complete deperturbation.

The choice of an adiabatic picture leads to difficulties when one of the potentials has a double minimum (see Fig. 3.5). The vibrational level separations of such a curve do not vary smoothly with vibrational quantum number, as do the levels of a single minimum potential. In the separate potential wells (below the barrier), the levels approximately follow two different smooth curves. However, above the potential barrier the separation between consecutive energy levels oscillates. The same pattern of behavior is found for the rotational constants below and above the potential barrier. In addition, the rotational levels above the barrier do not vary as $B_v J(J+1)$. An adiabatic deperturbation of the (E,F+G,K) $^1\Sigma_g^+$ states of H_2 has been possible (Dressler *et al.*, 1979) only because the adiabatic curves were known from very precise *ab initio* calculations.

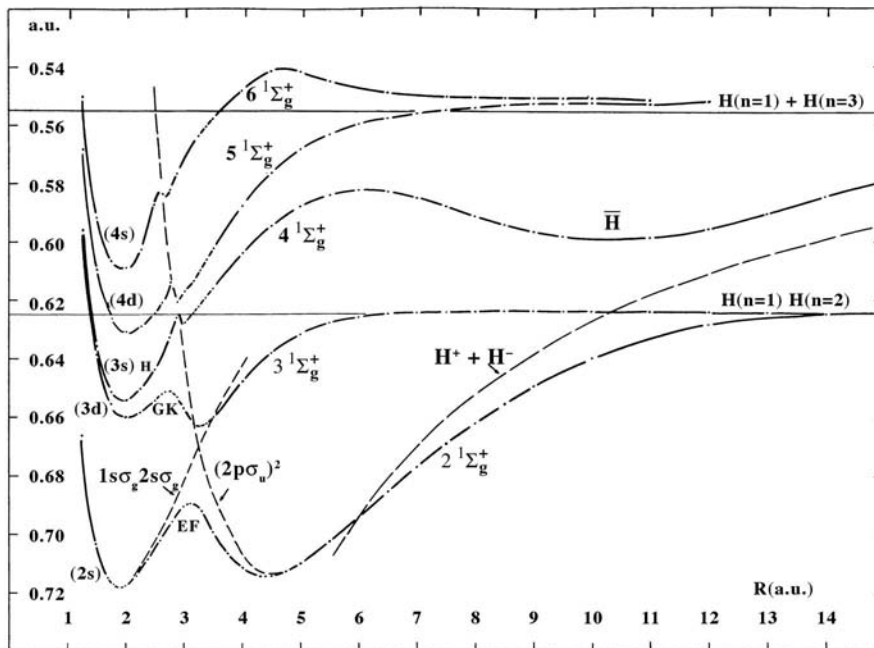


Figure 3.8: *Ab initio* adiabatic potential curves with double minima for the $1\Sigma_g^+$ states of H_2 (dash-dot line). The diabatic $1s\sigma_g 2s\sigma_g$ and $(2p\sigma_u)^2$ potentials are also plotted (dashed line). The (nl) labels on the small- R potential minima denote the dominant $1s\sigma_g nl\sigma_g$ configuration (Wolniewicz and Dressler, 1977). Note that more accurate results on the $4\ 1\Sigma_g^+$ H, $\bar{\text{H}}$ state have been presented by Wolniewicz and Dressler (1979) and by Dressler and Wolniewicz (1981).

If the approximate deperturbed curves do not cross or have similar spectroscopic constants, the most convenient starting point is an adiabatic approach. Two situations must be considered:

1. *The adiabatic curves result from an apparently avoided crossing.* This means that the diabatic curves belong to very different electronic configurations. The coupling matrix element, $W^e(R)$, can be assumed to have a Lorentzian shape [Eq. (3.3.14)]. This is the situation for the G and I states of SiO.

2. *The adiabatic curves correspond to configurations that differ by only one orbital.* Rydberg states belonging to series which converge to the same state of the ion fall into this category. Then the matrix element of $\partial/\partial R$ is generally R -independent (or linear in R).[†] One example is the perturbations observed between identical-symmetry Rydberg states of H_2 that converge to the same state of H_2^+ (the ground state) but to different vibrational levels of this state (Herzberg and Jungen, 1972). As the density of electronic levels increases near

[†] If the unique orbital changes its character with R (e.g., “Rydbergization”, Section 5.2.2), the coupling matrix element behaves similarly to case (1).

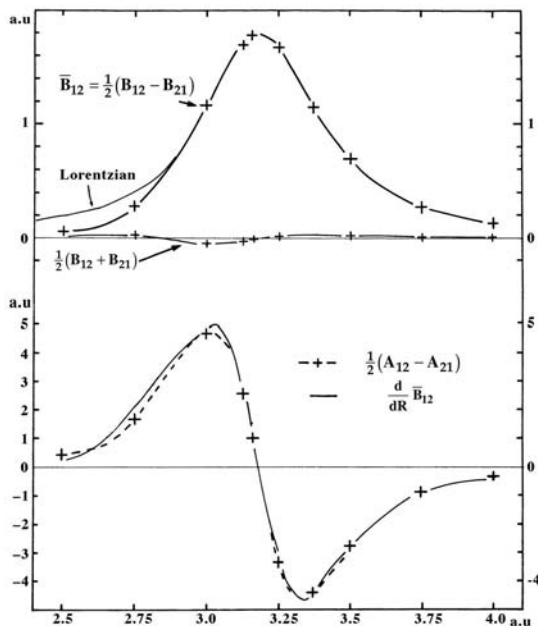


Figure 3.9: *Ab initio* $\partial/\partial R$ and $\partial^2/\partial R^2$ matrix elements between the E, F and G, K adiabatic states of H_2 : $B_{12} \equiv \langle \Phi_{1ad} | \frac{\partial}{\partial R} | \Phi_{2ad} \rangle_r$, $A_{12} \equiv \langle \Phi_{1ad} | \frac{\partial^2}{\partial R^2} | \Phi_{2ad} \rangle_r$ where Φ_1 and Φ_2 are the adiabatic electronic wavefunctions for the E, F and G, K double-minimum states, respectively. Except for the smallest R values, $\bar{B}_{12}(R)$ is Lorentzian. The relationships $B_{12} = -B_{21}$ and $\frac{1}{2}(A_{12} - A_{21}) = \frac{d}{dR}\bar{B}_{12}$ are not satisfied exactly because Φ_{1ad} and Φ_{2ad} are, in these calculations, not exactly orthogonal (Dressler, *et al.*, 1979).

the ionization limit, the $v = 1$ level of the ${}^1\Pi_u$ $n = 11$ Rydberg state is nearly degenerate with $v = 2$ of the ${}^1\Pi_u$ $n = 6$ Rydberg state (Fig. 3.10). The electronic factor is found to be nearly independent of R , $\langle \Phi_1^{ad} | \partial/\partial R | \Phi_2^{ad} \rangle_r = \text{constant}$. The vibrational wavefunctions of the two interacting states belong to virtually identical potentials; thus the vibrational factor is zero except for $\Delta v = 1$, which, in the harmonic approximation, is proportional to $(v + 1)^{1/2}$,

$$\left\langle \chi_{v_1} \left| \frac{\partial}{\partial R} \right| \chi_{v_2} \right\rangle (\text{\AA}^{-1}) = \left(\frac{\mu(\text{amu})\omega(\text{cm}^{-1})}{67.4304} \right)^{1/2} (v_1 + 1)^{1/2}, \quad (3.3.15)$$

with $v_2 = v_1 + 1$. Another approach to the treatment of these Rydberg~Rydberg interactions is given in Section 8.6, using, as zero-order electronic wavefunctions, those of a single electron in the field of the ion core (Jungen and Atabek, 1977).

The vibrational eigenstates of neither the diabatic nor the adiabatic potential curve exactly represent the observed levels. Interaction matrix elements between these zero-order levels (eigenstates of either diabatic or adiabatic potentials)

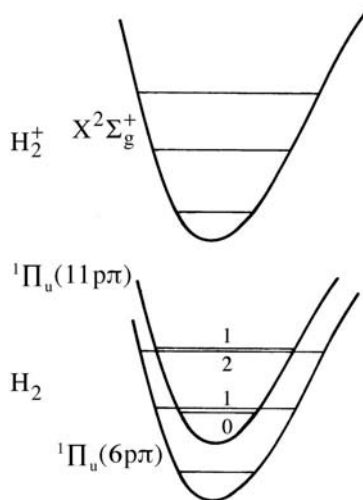


Figure 3.10: Perturbations between the $6p\pi$ and $11p\pi$ ${}^1\Pi_u$ Rydberg states of H_2 . Two Rydberg series converging to different vibrational levels of the H_2^+ $X^2\Sigma_g^+$ state interact via nonzero $\Delta v = \pm 1$ vibrational matrix elements of the $\partial/\partial R$ operator.

must be added in order to reproduce the observed levels. Table 3.6 summarizes the results of two types of deperturbation approaches, diabatic and adiabatic, to the same problem, a pair of interacting ${}^1\Pi$ states of SiO .

Recall that the purpose of a deperturbation calculation is to obtain a model, consisting of a pair of deperturbed potentials and an interaction matrix element (either R -dependent or R -independent), that exactly reproduces the observed rotation-vibration energy levels. Whether this model is diabatic or adiabatic has no effect on the quality of the agreement between observed and calculated levels. Where the two approaches differ is in the complexity of the calculation (size of matrix to be diagonalized, number of fitting iterations required, etc.) and in the magnitudes of the differences between observed and zero-order deperturbed levels (the eigenvalues of the deperturbed potentials). Table 3.6 displays the differences (obs - dep) between the observed levels (far right column), and the *zero-order* diabatic (second column) and *zero-order* adiabatic (fourth column) levels. The energies of the zero-order adiabatic levels are closer to those of the observed levels; thus the adiabatic picture is a better starting point for an iterative deperturbation calculation.

The observed levels in Table 3.6 may be obtained from the diabatic potentials represented by the T_e , ω_e , $\omega_e x_e$, and R_e constants, which generate the deperturbed levels via $T_v = T_e + \omega_e \left(v + \frac{1}{2}\right) - \omega_e x_e \left(v + \frac{1}{2}\right)^2$; an R -independent electronic matrix element, $H^e = 365 \text{ cm}^{-1}$; and vibrational overlap factors calculated using the vibrational eigenfunctions of the deperturbed diabatic potentials. Similarly, the observed levels may be computed from the adiabatic potentials, a Lorentzian interaction term [Eq. (3.3.14)] $W^e(R)$ with $b = 0.1014$

Table 3.6: Comparison between Two Types of Deperturbation of the G and I $^1\Pi$ States of SiO (in cm^{-1})

State	Diabatic deperturbation		Adiabatic deperturbation		Observed levels ^(a)
	Diabatic levels	obs - dep	Adiabatic levels	obs - dep	
G 0	70180	- 78	70099	3	70102
G 1	71056	- 91	70966	- 1	70965
G 2	71919	- 87	71819	13	71832
G 3	72769	-150	72658	-39	72619
G 4	73606	-163	73482	-39	73443
G 5	74431	-177	74292	-38	74254
G 6	75243	-192	75087	-36	75051
G 7	76042	-194	75866	-18	75848
I 0	71689	89	71788	-10	71778
I 1	72564	151	72675	40	72715
I 2	73423	170	73546	47	73593
I 3	74264	200	74401	63	74464
I 4	75089	236	75241	84	75325
I 5	75896	276	76066	106	76172

Spectroscopic constants for deperturbed curves (cm^{-1})^(b)

Diabatic curves	T_e	ω_e	$\omega_e x_e$	R_e (Å)
G	69,734.7	890.024	6.57	1.6139
I	71,245.0	892.014	8.66	1.6548

Interaction matrix element: $H^e = 365 \text{ cm}^{-1}$

Adiabatic curves	T_e	$\omega_e^{(c)}$	$\omega_e x_e^{(c)}$	R_e (Å)
G	69,633.0	881.07	7.02	1.6155
I	71,334.0	902.84	7.97	1.6526

Interaction matrix element:^(d) $b = 0.1014 \text{ \AA}$
 $R_C = 1.915 \text{ \AA}$ ^aLagerqvist and Renhorn, (1979)^bLefebvre-Brion (unpublished calculations, 1981).^cApproximate values, since the adiabatic levels are obtained by direct numerical integration of the adiabatic curves constructed from the diabatic curves and H^e .^dThe adiabatic interaction parameter, $W^e(R)$, is defined by Eq. (3.3.14) in terms of b and R_e .

Å, $R_C = 1.915$ Å, and vibrational factors calculated using eigenfunctions of the deperturbed adiabatic potentials.

Finally, the eigenfunctions for the observed levels are obtained, in either representation, by diagonalizing the complete interaction matrix consisting of all vibrational levels of the two potentials in the diabatic picture,

$$\Psi = \sum_{v_1} a_{v_1} \Phi_1^d \chi_{v_1}^d + \sum_{v_2} b_{v_2} \Phi_2^d \chi_{v_2}^d, \quad (3.3.16)$$

or, in the adiabatic picture,

$$\Psi = \sum_{v_1} c_{v_1} \Phi_1^{ad} \chi_{v_1}^{ad} + \sum_{v_2} d_{v_2} \Phi_2^{ad} \chi_{v_2}^{ad}. \quad (3.3.17)$$

Equations (3.3.16 and 3.3.17) suggest one final indicator of whether the diabatic or adiabatic approach is preferable. The better approach is the one for which the sum over deperturbed functions involves fewer terms, especially if one term is dominant (for example, $a_i \geq 2^{-1/2}$). An adiabaticity parameter

$$\gamma \equiv H^e / \Delta G^{ad}$$

has been introduced by Dressler (1983 and 1985), where ΔG^{ad} is the vibrational frequency of the higher-energy member of the pair of adiabatic electronic states. Near adiabatic behavior occurs for $\gamma \gg 1$; near diabatic behavior occurs for $\gamma \ll 1$. For $\gamma \simeq 1.0$, which corresponds to the case for the SiO G and I $^1\Pi$ states, the mixing of the vibrational basis functions is large in both diabatic and adiabatic descriptions.

3.3.5 Electromagnetic Field-Dressed Diabatic and Adiabatic Potential Energy Curves

Most of the experiments discussed in this book are performed using continuous wave or nanosecond-pulsed lasers at $I < 10^9$ W/cm² intensities, which correspond to electromagnetic radiation electric field strengths of $\mathcal{E} < 9 \times 10^5$ V/cm. Such electric fields are weak relative to typical intramolecular field strengths, $\mathcal{E}^0 = 1 a.u. = 5.14 \times 10^9$ V/cm and are appropriately treated perturbatively (see Sections 6.1.2 and 6.5.3).

When experiments are performed in the intense $I > 10^{11}$ W/cm² electromagnetic fields typically provided by picosecond or femtosecond pulsed lasers, it is necessary to solve the time-dependent Schrödinger equation in a non-perturbative approach (see Section 9.1.2). The total Hamiltonian is

$$\mathbf{H} = \mathbf{H}^0 + \vec{\mathcal{E}}(t) \cdot \left(\sum_i e \vec{r}_i \right) \quad (3.3.18)$$

where \mathbf{H}^0 is the field-free Hamiltonian of Eq. (3.1.1) and

$$\vec{\mathcal{E}}(t) = \hat{\mathbf{k}} \mathcal{E}^0 \cos \omega t \quad (3.3.19)$$

2. Electronic Configurations

It is usually possible and useful to assign observed molecular electronic states to electronic configurations. A configuration is a list of the molecular orbitals occupied by electrons. Molecular orbitals are usually specified by $n\ell\lambda$, where n is an integer > 1 , ℓ is the orbital angular momentum ($\ell = 0, 1, 2, 3, 4 \rightarrow s, p, d, f, g$), and λ is the projection of ℓ on the internuclear axis ($\lambda \leq \ell$, $\lambda = 0, 1, 2, 3, 4 \rightarrow \sigma, \pi, \delta, \phi, \gamma$). Two conventions exist for n , the molecular orbital convention attributes two sets of orbitals $\ell\lambda$ and $\ell\lambda^*$ for each value of n (bonding and antibonding*), the other more common convention simply numbers the $\ell\lambda$ orbitals in order of energy. Often (particularly for Rydberg states) n has the same meaning as the principal quantum number of atoms. The electron configuration is written by enclosing each orbital designation in parentheses and writing the occupancy as a right superscript. The $X^1\Sigma^+$ state of CO (14 electrons) belongs to the $(1s\sigma)^2(1s\sigma^*)^2(2s\sigma)^2(2s\sigma^*)^2(2p\sigma)^2(2p\pi)^4$ configuration. The maximum occupancy of a σ orbital is 2, of a π orbital 4, of a δ orbital 4, etc. Note that all orbitals for the CO $X^1\Sigma^+$ state are filled. Filled orbitals can give rise only to $^1\Sigma^+$ states. In working out molecular properties from 1-electron functions, the closed-shell core electrons are ignored. Note also that the molecular orbital picture describes CO as having a triple bond. Often configurations are abbreviated by omitting filled shells. Excited states of CO belong to the following configurations.

$$\begin{aligned} (2p\pi)^4(2p\sigma)(2p\pi^*) & \quad A^1\Pi, a^3\Pi, \\ (2p\pi)^3(2p\sigma)^2(2p\pi^*) & \quad a'^3\Sigma^+, e^3\Sigma^-, d^3\Delta, I^1\Sigma^-, D^1\Delta, ^1\Sigma^+ \end{aligned}$$

The reason L is undefined in molecules is illustrated by the above configuration labels: $2p\sigma \neq 2p\pi$, but in an atom $(2p\pi)(2p\sigma) \rightarrow (np)^2$ which gives rise to states with $L = 0, 1, 2$ and $S = 0, 1$. Thus, whenever more than 1 $\ell > 0$ electron is outside of a closed shell, there will be an essential ambiguity about L . L can be evaluated using *ab initio* wave functions to calculate the expectation value of \mathbf{L}^2 .

Usually, molecular states can be unambiguously assigned a configuration label. Although configuration mixing is always present, it is usually relatively small ($< 5\%$) and relatively independent of internuclear distance. In such cases, configuration labels are particularly useful in:

1. The analysis of perturbations – the magnitudes of perturbation interactions ($A_{\Pi\Sigma}\mathbf{L}_+$, $B_{\Pi\Sigma}\mathbf{L}_+$) for various perturbations may be related to each other or even to A_{Π} and B_{Π} .
2. Lambda doubling may be related to either B_{Π} and A_{Π} (pure precession) or $A_{\Pi\Sigma}\mathbf{L}_+$, $B_{\Pi\Sigma}\mathbf{L}_+$.
3. Properties of Rydberg states may be related to those of ionic states.
4. Additional selection rules for observability of perturbations are obtained and may be used to assign configuration labels to other states.

5. The sign of A_{Π} and $A_{\Pi,\Sigma}$ may be predicted.

A general method for construction of basis functions as products of 1-electron spin-orbitals is clearly described in The Theory of Atomic Spectra, pages 160-174, by E. U. Condon and G. H. Shortley. Wave functions which are antisymmetric with respect to interchange of electrons are compactly written as a determinant of 1-electron functions. The columns of the determinant correspond to the electron index, and the rows correspond to the occupied spin-orbitals. For example, a $(2p\pi)^2(2p\sigma)$ configuration has the following spin-orbitals (in standard order C & S, p. 169):

$$|n\lambda\sigma\rangle = (2p1^+)(2p1^-)(2p-1^+)(2p-1^-)(2p0^+)(2p0^-)$$

The \pm right superscript refers to the electron spin $\pm\frac{1}{2}$. To write a determinantal function corresponding to a particular state of the $\pi^2\sigma$ configuration one picks the three spin-orbitals needed to obtain the desired Λ , Σ , Ω . The states derived from $\pi^2\sigma$ are ${}^2\Sigma^+$, ${}^2\Sigma^-$, ${}^2\Delta$, ${}^4\Sigma^-$.

$${}^2\Delta_{5/2} = \frac{1}{\sqrt{3!}} \begin{vmatrix} 2p1^+(1) & 2p1^+(2) & 2p1^+(3) \\ 2p1^-(1) & 2p1^-(2) & 2p1^-(3) \\ 2p0^+(1) & 2p0^+(2) & 2p0^+(3) \end{vmatrix}$$

Using a shorthand, we drop the $2p$ and write only the three diagonal functions. The procedure for assigning the various determinants to $|\Lambda S \Sigma\rangle$ basis functions is laborious. First write all determinants for each value of Λ and Σ .

$$\begin{array}{llll} \Lambda = 2, & \Sigma = \frac{1}{2} & \||1^+(1) 1^-(2) 0^+(3)\| & {}^2\Delta_{3/2} \\ \Lambda = 2, & \Sigma = -\frac{1}{2} & \||1^+(1) 1^-(2) 0^-(3)\| & {}^2\Delta_{1/2} \\ \Lambda = 0, & \Sigma = \frac{3}{2} & \||1^+(1) - 1^+(2) 0^+(3)\| & {}^4\Sigma_{3/2}^- \\ \Lambda = 0, & \Sigma = \frac{1}{2} & \left\{ \begin{array}{l} \||1^+(1) - 1^+(2) 0^-(3)\| \\ \||1^+(1) - 1^-(2) 0^+(3)\| \\ \||1^-(1) - 1^+(2) 0^+(3)\| \end{array} \right\} & {}^4\Sigma_{1/2}, {}^2\Sigma^+, {}^2\Sigma^- \end{array}$$

Omit negative values of Λ . There is an ambiguity for $\Lambda = 0$, $\Sigma = \frac{1}{2}$. We use \mathbf{S}_- and σ_v to assign the

remaining three functions to ${}^2\Sigma^+$, ${}^2\Sigma^-$, ${}^4\Sigma_{1/2}^-$

$$\begin{aligned}\mathbf{S}_- |{}^4\Sigma_{3/2}^- \rangle &= [(S + \Sigma)(S - \Sigma + 1)]^{1/2} |{}^4\Sigma_{1/2}^- \rangle \\ |{}^4\Sigma_{1/2}^- \rangle &= (3)^{-1/2} \mathbf{S}_- |{}^4\Sigma_{3/2}^- \rangle \\ \mathbf{S}_- &= \sum_{i=1}^3 \mathbf{s}_i^-.\end{aligned}$$

Thus

$$\begin{aligned}|{}^4\Sigma_{1/2}^- \rangle &= (3)^{-1/2} \sum_{i=1}^3 \mathbf{s}_i^- \|1^+(1) - 1^+(2) 0^+(3)\| \\ &= (3)^{-1/2} [\|1^- - 1^+0^+\| + \|1^+ - 1^-0^+\| + \|1^+ - 1^+0^-\|]\end{aligned}$$

Since $\mathbf{s}_- |s = \frac{1}{2}, \sigma = \frac{1}{2}\rangle = \left[\left(\frac{1}{2} + \frac{1}{2}\right)\left(\frac{1}{2} - \frac{1}{2} + 1\right)\right]^{1/2} = 1$.

We know doublet functions must be orthogonal to quartet so try

$$\begin{cases} \|1^- - 1^+0^+\| - \|1^+ - 1^-0^+\| \\ -\|1^- - 1^+0^+\| - \|1^+ - 1^-0^+\| + 2\|1^+ - 1^+0^-\| \end{cases}$$

and observe effect of σ_v on these mutually orthogonal functions.

$$\begin{aligned}\sigma_v^\lambda |\ell\lambda\rangle &= (-1)^{\ell-\lambda} |\ell - \lambda\rangle, \ell = 1 \\ \sigma_v^\Lambda |L\Lambda\rangle &= \pm(-1)^{L-\Lambda} |L - \Lambda\rangle, L \equiv 2 \text{ arbitrarily chosen} \\ \sigma_v^\Lambda |{}^2\Sigma^+\rangle &= + |{}^2\Sigma^+\rangle \\ \sigma_v^\Lambda |{}^2\Sigma^-\rangle &= - |{}^2\Sigma^-\rangle \\ \sigma_v^\Lambda &= \prod_i \sigma_{vi}^\lambda\end{aligned}$$

$$\begin{aligned}\sigma_{v1}^\lambda \sigma_{v2}^\lambda \sigma_{v3}^\lambda [\|1^- - 1^+0^+\| - \|1^+ - 1^-0^+\|] &= (-1)^{0+2+1} \| - 1^-1^+0^+\| - (-1)^{0+2+1} \| - 1^+1^-0^+\| \\ &= (-1)[\| - 1^-1^+0^+\| - \| - 1^+1^-0^+\|]\end{aligned}$$

but the two determinants are not in standard order. An interchange of adjacent columns results in a sign change. Thus

$$\begin{aligned}\sigma_v^\Lambda [\|1^- - 1^+0^+\| - \|1^+ - 1^-0^+\|] &= [\|1^+ - 1^-0^+\| - \|1^- - 1^+0^+\|] \\ &= (-1)[\|1^- - 1^+0^+\| - \|1^+ - 1^-0^+\|]\end{aligned}$$

Thus the function belongs to ${}^2\Sigma^-$.

$$\text{So } {}^2\Sigma_{1/2}^- = 2^{-1/2}[\|1^- - 1^+0^+\| - \|1^+ - 1^-0^+\|]$$

$$\text{and } {}^2\Sigma_{1/2}^+ = 6^{-1/2}[2\|1^+ - 1^+0^-\| - \|1^- - 1^+0^+\| - \|1^+ - 1^-0^+\|]$$

So we have explicitly written out all the states of the $(2p\pi)^2(2p\sigma)$ configuration. Now consider the states of the $(2p\pi)(2p\sigma)^2$ configuration. There is only a ${}^2\Pi$ state.

$${}^2\Pi_{3/2} = \|1^+0^+0^-\|$$

$${}^2\Pi_{1/2} = \|1^-0^+0^-\|.$$

How do we take matrix elements using these functions? The usual operators may be re-written in terms of 1-electron or 2-electron operators.

$$\underline{A}\mathbf{L} \cdot \mathbf{S} \equiv \sum_i a_i \boldsymbol{\ell}_i \cdot \mathbf{s}_i = \sum_i a_i \left[\ell_{iz} s_{iz} + \frac{1}{2} (\boldsymbol{\ell}_{i+} \mathbf{s}_{i-} + \boldsymbol{\ell}_{i-} \mathbf{s}_{i+}) \right].$$

Note that this form of $\underline{A}\mathbf{L} \cdot \mathbf{S}$ has $\Delta S = 0, \pm 1$ selection rule.

$$B\mathbf{L} \cdot \mathbf{S} = B \left(\sum_i \boldsymbol{\ell}_i \right) \cdot \left(\sum_i \mathbf{s}_j \right).$$

Note that this form of $B\mathbf{L} \cdot \mathbf{S}$ has exclusively the $\Delta S = 0$ selection rule.

$$\mathbf{J} \cdot \mathbf{L} = \mathbf{J} \cdot \sum_i \boldsymbol{\ell}_i$$

$$\mathbf{J} \cdot \mathbf{S} = \mathbf{J} \cdot \sum_i \mathbf{s}_i.$$

These operators should give exactly the same matrix elements we obtained using $|\Omega JM\rangle | \Lambda S \Sigma \rangle$ functions.

Consider $\langle {}^2\Pi_{1/2} | \underline{A}\mathbf{L} \cdot \mathbf{S} | {}^2\Sigma_{1/2}^- \rangle$. A 1-electron operator can have nonzero matrix elements between product functions differing by no more than 1 spin-orbital. In addition, no 1-electron angular momentum operator can change n (principal quantum number). Thus we have a new selection rule for perturbations. This is what is meant by configurationally forbidden perturbations. Configurationally forbidden perturbations are:

1. $\Delta n \neq 0$
2. Or involve states belonging to configurations differing by more than one orbital.

How do we evaluate matrix elements? (C & S, p. 169-171).

$$\begin{aligned} \langle {}^2\Pi_{1/2} | \mathbf{A}\mathbf{L} \cdot \mathbf{S} | {}^2\Sigma_{1/2}^- \rangle &= 2^{-1/2} \left\langle \left\| 1^- 0^+ 0^- \left\| \sum_{i=1}^3 \frac{1}{2} a_i \boldsymbol{\ell}_{i+} \mathbf{s}_{i-} \right\| 1^- - 1^+ 0^+ \right\| \right\rangle \\ &= -2^{-1/2} \left\langle \left\| 1^- 0^+ 1^- \left\| \sum_{i=1}^3 \frac{1}{2} a_i \boldsymbol{\ell}_{i+} \mathbf{s}_{i-} \right\| 1^+ - 1^- 0^+ \right\| \right\rangle. \end{aligned}$$

The locations of the identical spin-orbitals in the left- and right-hand functions must agree and the pair of differing spin-orbitals must also be at the same location. The right-hand function in the first term must be rearranged by a switch of -1^+ and 0^+ to match the left-hand function. The second term cannot be rearranged because the left and right functions differ by two spin-orbitals.

Thus

$$\langle {}^2\Pi_{1/2} | \mathbf{A}\mathbf{L} \cdot \mathbf{S} | {}^2\Sigma_{1/2}^- \rangle = -2^{-1/2} \left\langle \left\| 1^- 0^+ 1^- \left\| \sum_{i=1}^3 \frac{a_i}{2} \boldsymbol{\ell}_{i+} \mathbf{s}_{i-} \right\| 1^- 0^+ - 1^+ \right\| \right\rangle.$$

The first two terms in the summation over i are zero, because the difference between the left and right functions is in the third spin-orbital and $\boldsymbol{\ell}_+ \mathbf{s}_-$ causes a change in spin-orbital.

$$\begin{aligned} \langle {}^2\Pi_{1/2} | \mathbf{A}\mathbf{L} \cdot \mathbf{S} | {}^2\Sigma_{1/2}^- \rangle &= -2^{-3/2} \langle 0^- | a \boldsymbol{\ell}_+ \mathbf{s}_- | -1^+ \rangle \\ &= -2^{-3/2} \langle 0 | a \boldsymbol{\ell}_+ | -1 \rangle \left\langle -\frac{1}{2} | \mathbf{s}_- | \frac{1}{2} \right\rangle \\ &= -2^{-3/2} \langle 0 | a \boldsymbol{\ell}_+ | -1 \rangle \left[\left(\frac{1}{2} + \frac{1}{2} \right) \left(\frac{1}{2} - \frac{1}{2} + 1 \right) \right]^{1/2} \\ &= -2^{-3/2} \langle 0 | a \boldsymbol{\ell}_+ | -1 \rangle. \end{aligned}$$

Often, because ℓ is usually not a good quantum number, only the \mathbf{s}_- part of the matrix element is evaluated. If ℓ is good, then

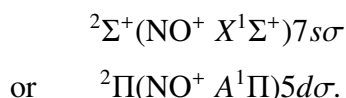
$$\begin{aligned} \langle {}^2\Pi_{1/2} | \mathbf{A}\mathbf{L} \cdot \mathbf{S} | {}^2\Sigma_{1/2}^- \rangle &= -2^{-3/2} \langle 0 | \boldsymbol{\ell}_+ | -1 \rangle \langle n = 2 | a | n = 2 \rangle \\ &= -2^{-3/2} [(1+1)(1-1+1)]^{1/2} \langle n = 2 | a | n = 2 \rangle. \end{aligned}$$

$n = 2$ because we started with $2p\pi$, $2p\sigma$ orbitals. All matrix elements involving the $(2p\pi)$ $(2p\sigma)^2$ ${}^2\Pi$ state and the $(2p\pi)^2(2p\sigma)^2$ ${}^2\Sigma^+$, ${}^2\Sigma^-$, ${}^4\Sigma^-$, ${}^2\Delta$ states can be re-expressed in terms of matrix elements of the form

$$\begin{aligned} &\langle n = 2, \ell = 1, \lambda = 1 | a \boldsymbol{\ell}_+ | n = 2, \ell = 1, \lambda = 0 \rangle \\ &B \langle n = 2, \ell = 1, \lambda = 1 | \boldsymbol{\ell}_+ | n = 2, \ell = 1, \lambda = 0 \rangle \end{aligned}$$

and thus the magnitudes of all such perturbations can be inter-related. If the $\ell\lambda$ labels used to describe the configuration are not exact, these matrix elements indicate what the approximate value of ℓ is for a valence or a Rydberg orbital.

A Rydberg orbital is a diffuse atomic-like, nearly spherical orbital. Usually n and ℓ are good quantum numbers for Rydberg orbitals. The nuclei and inner orbitals look a “fat proton” to an electron in a Rydberg orbital. The “fat proton” looks to the spectroscopist like one of the electronic states of the corresponding ion, in fact a molecule in a Rydberg state has $B(v)$ and $G(v)$ functions nearly identical to those of the ionic state at the Rydberg series limit. The Rydberg series limit corresponds to $n = \infty$. Rydberg states are usually specified by writing the state of the ionic core, followed by the quantum numbers of the Rydberg orbital. For example, in NO



The states in a Rydberg series form a progression

$$E_n = T_\infty - \frac{R}{(n - \delta)^2}$$

where T_∞ is the series (ionization) limit and δ is the quantum defect. δ is usually small (less than 1) and is not quite constant. Note that Rydberg states have vibrational levels, but often only $v = 0$ is observed.

A valence orbital is compact, and n and ℓ are usually not good quantum numbers. A valence orbital is perfectly well specified by n, ℓ, λ , but one should regard these quantum numbers as labels only. Valence orbitals are usually lower in energy than Rydberg orbitals and higher in energy than the core orbitals. Valence states usually have longer r_e and smaller ω_e than either Rydberg states, ionic states, or the ground state.

Due to the goodness of the n, ℓ quantum numbers for Rydberg states, perturbations, lambda-doubling, and diagonal rotational constants and spin-orbit constants are all closely inter-related and easily understood. Since all Rydberg states belonging to the same series have similar potential curves, Franck-Condon factors involving two Rydberg states are usually $\langle v|v'\rangle = \delta_{vv'}$, and $\frac{\hbar^2}{2\mu} \langle v|\frac{1}{r^2}|v'\rangle = B_e \times \left[\delta_{vv'} - \frac{2x}{r_e} \delta_{vv'\pm 1} + \frac{6x^2}{r_e^2} - \dots \right]$ $x = r - r_e$ where x is the vibrational displacement coordinate appropriate for evaluating vibrational matrix elements in the harmonic oscillator basis set. This means that all second order constants of the form

$$\alpha\beta(\Pi\Sigma) = \sum_{v'} \frac{\langle v, {}^2\Pi | \mathbf{A}\mathbf{L}_+ | v', {}^2\Sigma \rangle \langle v, {}^2\Pi | \mathbf{B}\mathbf{L}_+ | v', {}^2\Sigma \rangle}{E_\Pi - E_\Sigma(v')}$$

simplify immediately to

$$\alpha\beta(\Pi\Sigma) = \frac{A_\Pi[(\ell - \lambda)(\ell + \lambda + 1)]^{1/2} B_\Pi[(\ell - \lambda)(\ell + \lambda + 1)]^{1/2}}{T_\Pi - T_\Sigma}$$

Thus

$$\alpha\beta(\Pi\Sigma) = \frac{A_{\Pi}B_{\Pi}\ell(\ell + 1)}{T_{\Pi} - T_{\Sigma}}$$

Similarly

$$\beta(\Pi\Sigma)^2 = \frac{B_{\Pi}^2\ell(\ell + 1)}{T_{\Pi} - T_{\Sigma}}.$$

This state of affairs is called “pure precession.” This occurs whenever n, ℓ are good quantum numbers. Rydberg states and most electronic states of hydrides are well described by pure precession. For valence states, when n, ℓ are not good quantum numbers, but are still good labels, a generalized pure precession result is obtained. Using the one electron product functions, all perturbation matrix elements and most second order sums may be accounted for by two constants

$$a \equiv \langle n\ell\lambda | a\ell_+ | n\ell\lambda - 1 \rangle$$

$$b \equiv \langle n\ell\lambda | \ell_+ | n\ell\lambda - 1 \rangle.$$

The second order sums do not reduce as easily as for pure precession, because the potential curves do not always have the same shape and r_e . Sums over

$$\sum_{v'} \frac{\langle v | v' \rangle}{E_{\Pi}(v) - E_{\Sigma}(v')} \quad \text{and} \quad \sum_{v'} \frac{\langle v, \Pi | B | v', \Sigma \rangle}{E_{\Pi}(v) - E_{\Sigma}(v')}$$

must be evaluated by computer.